MEMORANDUM REPORT ARBRL-MR-03295

A SIMPLE THEORETICAL ANALYSIS AND EXPERIMENTAL INVESTIGATION OF BURNING PROCESSES FOR STICK PROPELLANT

Frederick W. Robbins
Albert W. Horst

July 1983

US ARMY ARMAMENT RESEARCH AND DEVELOPMENT COMMAND
BALLISTIC RESEARCH LABORATORY
ABERDEEN PROVING GROUND, MARYLAND

UNCLASSIFIED

SECURITY CLASSIFICATION OF THIS PAGE (When Data Entered)

REPORT DOCUMENTATION PAGE		READ INSTRUCTIONS BEFORE COMPLETING FORM
1. REPORT NUMBER MEMORANDUM REPORT ARBRL-MR-03295	2. GOVT ACCESSION NO.	3. RECIPIENT'S CATALOG NUMBER
4. TITLE (and Subtitle) A SIMPLE THEORETICAL ANALYSIS AND EXPERIMENTAL INVESTIGATION OF BURNING PROCESSES FOR STICK PROPELLANT		5. TYPE OF REPORT & PERIOD COVERED October 1980 - September 1981 6. PERFORMING ORG. REPORT NUMBER
7. AUTHOR(s) F. W. Robbins A. W. Horst		8. CONTRACT OR GRANT NUMBER(s)
9. PERFORMING ORGANIZATION NAME AND ADDRESS US Army Ballistic Research Laboratory ATTN: DRDAR-BLI Aberdeen Proving Ground, MD 21005		10. PROGRAM ELEMENT, PROJECT, TASK AREA & WORK UNIT NUMBERS 1L162618AH80
11. CONTROLLING OFFICE NAME AND ADDRESS US Army Armament Research & Development Command US Army Ballistic Research Laboratory (DRDAR-BLA-S) Aberdeen Proving Ground, MD 21005		12. REPORT DATE July 1983 13. NUMBER OF PAGES 33
14. MONITORING AGENCY NAME & ADDRESS(if different from Controlling Office)		15. SECURITY CLASS. (of this report) Unclassified 15a. DECLASSIFICATION/DOWNGRADING SCHEDULE

16. DISTRIBUTION STATEMENT (of this Report)

Approved for public release; distribution unlimited.

17. DISTRIBUTION STATEMENT (of the abstract entered in Block 20, if different from Report)

18. SUPPLEMENTARY NOTES

19. KEY WORDS (Continue on reverse side if necessary and identify by block number)

Interior Ballistics
Stick Propellants
Burning Rate
Propellant Mechanical Properties

20. ABSTRACT (Continue on reverse side if necessary and identify by block number) nlg

The interior ballistic performance of propelling charges employing perforated unslotted stick propellant often cannot be simulated using either lumped-parameter or two-phase flow models without altering input data beyond realistic limits. In this work, a lumped-parameter model has been modified to account for enhanced burning within the perforations of stick propellant, a consequence of higher local pressures accompanying the choking of product gases exiting the perforations. A further extension allows treatment of

DD FORM 1 JAN 73 1473 EDITION OF 1 NOV 65 IS OBSOLETE

UNCLASSIFIED

SECURITY CLASSIFICATION OF THIS PAGE (When Data Entered) additional surface area exposed should grain fracture occur as a result of excessive internal pressures. Results obtained using the modified code are compared to 155-mm howitzer firings. Data from closed-bomb firings which demonstrate the same effect are also included.

TABLE OF CONTENTS

LIST OF ILLUSTRATIONS

LIST OF TABLES

I. INTRODUCTION

Stick propellant is finding increasing application in high-performance artillery charges. Currently employed in a number of European top-zone propelling charges, stick propellant is now being introduced into US artillery as a product improvement to the existing 155-mm, M203 (Zone 8S) Propelling Charge. Further, its use is all but assured in future advanced artillery systems under consideration in the United States.

The current popularity enjoyed by stick propellant can be attributed to a number of very desirable ballistic advantages associated with its use, some of them only potential but others clearly demonstrated. The natural flow channels associated with bundles of sticks reduce the resistance offered to the tortuous path required of flow through a granular propellant bed.[1] Locally high pressure gradients cannot therefore be supported in a stick propellant charge, and potentially damaging longitudinal pressure waves are all but unseen. In addition, the regular packing of propellant sticks yields higher loading densities than for randomly packed granular propellant, allowing equivalent performance with stick propellant charges using a slightly increased mass of lower energy, lower-flame-temperature propellant formulation. It is widely purported, and not unreasonable to expect, that the lower flame temperature should lead to increased barrel life and perhaps reduced muzzle flash and blast. Alternatively, a larger possible charge mass of the existing formulation may allow performance increases in an otherwise volume-limited gun system. With such worthwhile benefits in the offing, exploitation of the stick propellant concept certainly appears well-motivated.

In this paper, we address the task of modeling stick propellant performance in the 155-mm, M198 Howitzer. The application of classical charge design techniques involves the use of a lumped-parameter, interior ballistic code to determine the appropriate propellant geometry - particularly web, assuming a given grain configuration - required to achieve a desired performance level with a particular propellant formulation. An iterative procedure is generally followed, in which the web is incremented and resulting performance calculated until desired results are achieved. The technique often makes use of closed-bomb burning rate data, and when coupled with a form function relating burning surface (or fraction burned) to distance burned allows determination of mass (i.e., gas) generation rates needed to drive the interior ballistic cycle. This technique, when applied to conventional (e.g., single- or seven-perforation granular) propellant geometries, usually provides a quite satisfactory link between propellant web and the two major interior ballistic parameters - maximum chamber pressure and projectile muzzle velocity. However, the same technique applied to stick propellant has consistently led to higher than predicted maximum pressures in actual gun

[1] *F. W. Robbins, J. A. Kudzal, J. A. McWilliams, and P. S. Gough, "Experimental Determination of Stick Charge Flow Resistance," 17th JANNAF Combustion Meeting, CPIA Publication 329, Vol II, pp 97-118, November 1980.*

firings.[1-5] This disparity between theory and experiment is on the order of 5-10 percent for slotted sticks and as much as 25 percent for long, unslotted sticks with small perforations. The need for a rational and cost-effective design methodology for stick propellant charges mandates an improvement in our modeling capability.

The lumped-parameter, interior ballistic code used in this study is a modified version of the Baer-Frankle computer code.[6] The modification consists of decoupling of the burning in the perforation and interfacing it to the rest of the problem by subsonic and sonic pipe-flow equations. The two-phase flow code is an experimental version of the NOVA code,[7] developed by Paul Gough Associates for the Naval Ordnance Station, Indian Head, MD, in which burning in the perforation is treated separately from the rest of the problem and given an independent continuum representation.

II. EXPERIMENTAL

A. Comparative 155-mm Howitzer Firings

Baseline firings were first conducted in a 155-mm howitzer (M199 Cannon) at the Ballistic Research Laboratory's Sandy Point (R-18) Test Facility. Ballistically equivalent (i.e., same muzzle velocities) propelling charges employing (1) standard 7-perforated, granular, (2) single-perforated, slotted stick, and (3) single-perforated, unslotted stick, M30A1 propellant were employed. The granular propellant charges were constructed by down-loading standard M203 Propelling Charges, Lot IND-78F-069805, and employed the standard centercore ignition system. The stick charges were constructed using

---

[2] *T. C. Smith, "Experimental Gun Testing of High Density Multi-Perforated Stick Propellant Charge Assemblies," 17th JANNAF Combustion Meeting, CPIA Publication 329, Vol II, pp 87-98, November 1980.*

[3] *A. Grabowsky, S. Weiner, and A. Beardell, "Closed Bomb Testing of Stick Propellant for Gun Firing Simulation," 17th JANNAF Combustion Meeting, CPIA Publication 329, Vol II, pp 119-124, November 1980.*

[4] *A. W. Horst and T. C. Minor, "Improved Flow Dynamics in Guns Through the Use of Alternative Propellant Grain Geometries," 1980 JANNAF Propulsion Meeting, CPIA Publication 315, Vol I, pp 325-352, March 1980.*

[5] *S. Weiner, "Investigation of Stick Propellant for 155-mm Howitzer XM198," Interim Memorandum Report, Picatinny Arsenal, Dover, New Jersey, July 1975.*

[6] *P. G. Baer and J. M. Frankle, "The Simulation of Interior Ballistic Performance of Guns by Digital Computer Program," BRL R 1183, USA Aberdeen Research and Development Center, Ballistic Research Laboratories, Aberdeen Proving Ground, MD, December 1962 (AD 299980).*

[7] *P. S. Gough, "Extensions to NOVA Flamespreading Modeling Capacity," Task I Report for Naval Ordnance Station, Indian Head, MD, Contract N00174-80-C-0316, Paul Gough Associates, Inc., Portsmouth, NH, April 1981.*

Table 1. Firing Results for Three Propellant Configurations

Propellant Type	Propellant Mass kg (lb) Average	Range	Maximum Pressure MPa (kpsi) Average	Range	Muzzle Velocity m/s (f/s) Average	Range	Grain Dimensions* - mm(in.) Length	Perforation Diameter	Outside Diameter	Web
Granular, 7-Perforated, Propellant Lot RAD-77G-069805	11.55 (24.47)**		322 (46.6)	28 (4.1)	814 (2670)	12 (39)	24.08 (0.9481)	0.858 (0.0338)	10.60 (0.4173)	2.03 (0.0800)
Stick, 1-Perforated, Slotted, Propellant Lot RAD-PE-472-11	10.85 (23.92)	0.01 (0.02)	310 (45.0)	5 (0.7)	814 (2670)	4 (13)	686.0 (27.01)	1.55 (0.0611)	6.571 (0.2587)	2.51 (0.0988)
Stick, 1-Perforated, Unslotted, Propellant Lot RAD-PE-472-12	10.34 (22.80)	0.01 (0.02)	357 (51.8)	0.0 (0.0)	817 (2680)	0.0 (0.0)	686.6 (27.03)	1.30 (0.0511)	6.347 (0.2499)	2.52 (0.0994)

* Grain dimensions from Propellant Specification Sheets
** Reported value (not measured)

Table 2. Firing Results for Three Lengths of Unslotted, Stick Propellant

Measured Grain Length mm (in.)	Maximum Pressure MPa (kpsi) Average	Range	Muzzle Velocity m/s (f/s) Average	Range
686 (27.0)	354 (51.3)		813 (2670)	
343 (13.5)	314 (45.5)	5 (0.8)	799 (2620)	2 (6)
171 (6.75)	263 (38.1)	3 (0.4)	778 (2550)	5 (16)

basepad igniters containing 57 g (2 oz) of CBI and a 14-g (1/2-oz) spot of black powder. Three replicates of each configuration were fired, all on the same day. A summary of firing results is provided in Table 1. As reported previously,[4] an apparent increase in thermodynamic efficiency is seen to accompany use of the stick propellant configurations. Further, the unslotted stick shows an even greater deviation from classically predicted levels than did the slotted stick, though the slotted and unslotted stick propellants had virtually identical webs.

A second set of howitzer firings was conducted using the unslotted stick propellant from above but cut to different lengths. A single firing of the uncut propellant and two firings each of half-length and one-fourth-length sticks were included. Results are summarized in Table 2. While classical ballistics would predict virtually identical results for all three configurations, we note a dramatic dependence of pressure and velocity on the length of the propellant sticks. This result will be discussed further in the section on analysis.

B. Propellant-Fracture Tests

Propellant fracture is an important potential mechanism for increasing burning surface beyond that predicted by classical pictures of burning. In order to assess its role in the process of stick propellant combustion, a number of tests were performed using various stick propellants subjected to internal pressurization.

In the first series of tests, both ends of propellant full-length sticks were epoxy-cemented into steel tubes, one end being sealed and the other flare-fitted to a regulator controlling a 21-MPa (3-kpsi) source of nitrogen gas. The perforations were slowly pressurized until grain fracture occurred. It should be noted that the first test using M30A1 propellant involved intermittent increases in pressure while the second was characterized by a continuous increase until fracture. Results are shown in Table 3.

Table 3. Failure Levels for Stick Propellant Samples Undergoing Slow Pressurization of the Perforation

	Test	Maximum Pressure MPa (psi)
M30A1 Propellant, Lot RAD-PE-472-12	#1	8.6 (1250)
	#2	12.4 (1800)
NOSOL 363 Propellant, Sample 1	#1	2.8 (400)
	#2	2.8 (400)

An attempt was then made to obtain similar data for propellant samples undergoing rapid pressurization of the perforation. Open-air tests were conducted for the three lengths of M30A1 propellant sticks (Lot RAD-PE-472-12), outside-inhibited, using a single pellet of black powder and an M100 electric match taped to each end. Internal pressures were thus rapidly generated by the burning perforation surface itself. The full length sticks burned for about a second, split along the axis with the ends usually intact, and extinguished. Similar results were obtained for the half-length sticks, while the one-fourth-length sticks apparently burned to completion.

To obtain quantitative data, full-length M30A1 sticks were then instrumented with pressure gages as shown in Figure 1, ignited with the black powder pellets/matches as above, but with and without confinement of the ends of the sticks in the aluminum blocks pictured. Recorded pressure-time curves are shown in Figures 2 and 3, with a summary of fracture pressures (defined as point where pressure drops quickly to zero) provided in Table 4. While the unconfined stick behaved as above, the samples with ends inserted in the aluminum blocks fractured completely, leaving no large pieces.

Table 4. Failure Levels for Stick Propellant Undergoing Dynamic Pressurization of the Perforation

	Position mm (in.)	Maximum Pressure MPa (psi)
Unconfined Ends:	86 (3.4)	27.4 (3970)
	171 (6.75)	33.5 (4860)
Confined Ends:	86 (3.4)	28.5 (4130)
	171 (6.75)	51.5 (7470)
	343 (13.5)	38.7 (5610)

C. Closed-Bomb Tests

Additional information was obtained from a series of closed-bomb firings employing NOSOL 363 propellant supplied by the Naval Ordnance Station, Indian Head, MD. Two, single-perforated granulations (Sample 1: outer diameter = 6.50 mm (0.265 in.), perforation diameter = 0.94 mm (0.037 in.); Sample 2: outer diameter = 7.62 mm (0.300 in.), perforation diameter = 2.13 mm (0.084 in.)) in each of four lengths (19 mm (0.75 in.), 83.8 mm (3.3 in.), 167 mm (6.6 in.), and 337 mm (13.25 in.)) were tested in a 700-cc bomb using black powder as the igniter material. Burning rates at 69 MPa (10 kpsi) and 207 MPa (30 kpsi) are plotted in Figure 4.

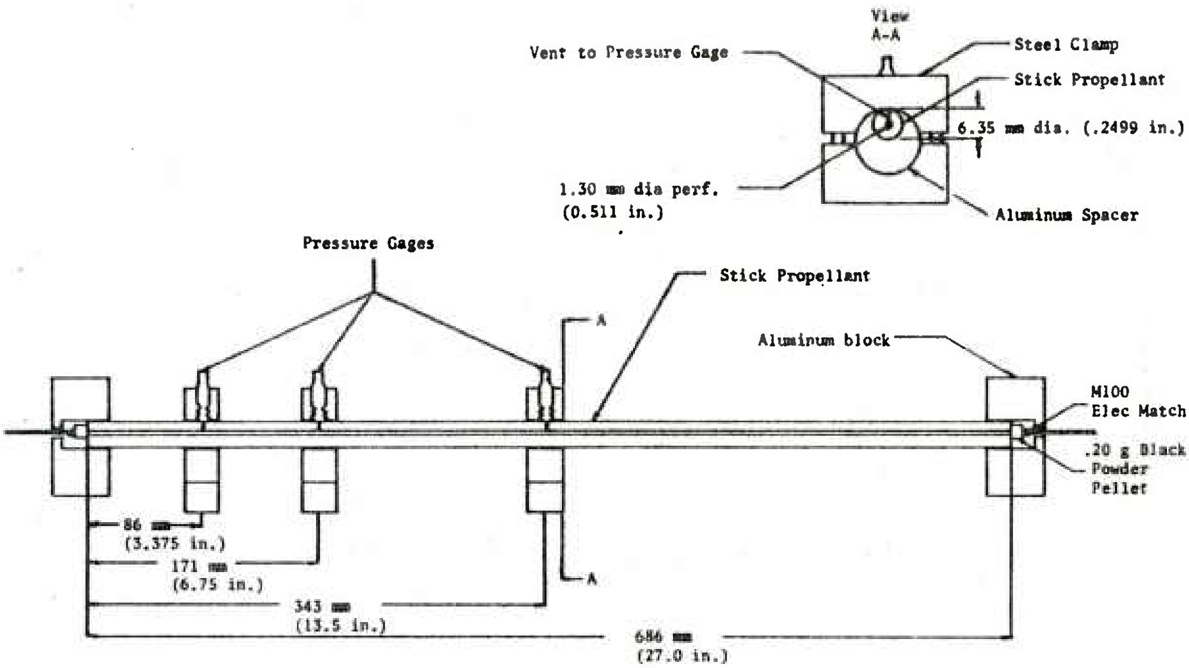

Figure 1. Experimental Setup for Measuring Pressures in the Burning Perforation of Single-Perforated Stick Propellant

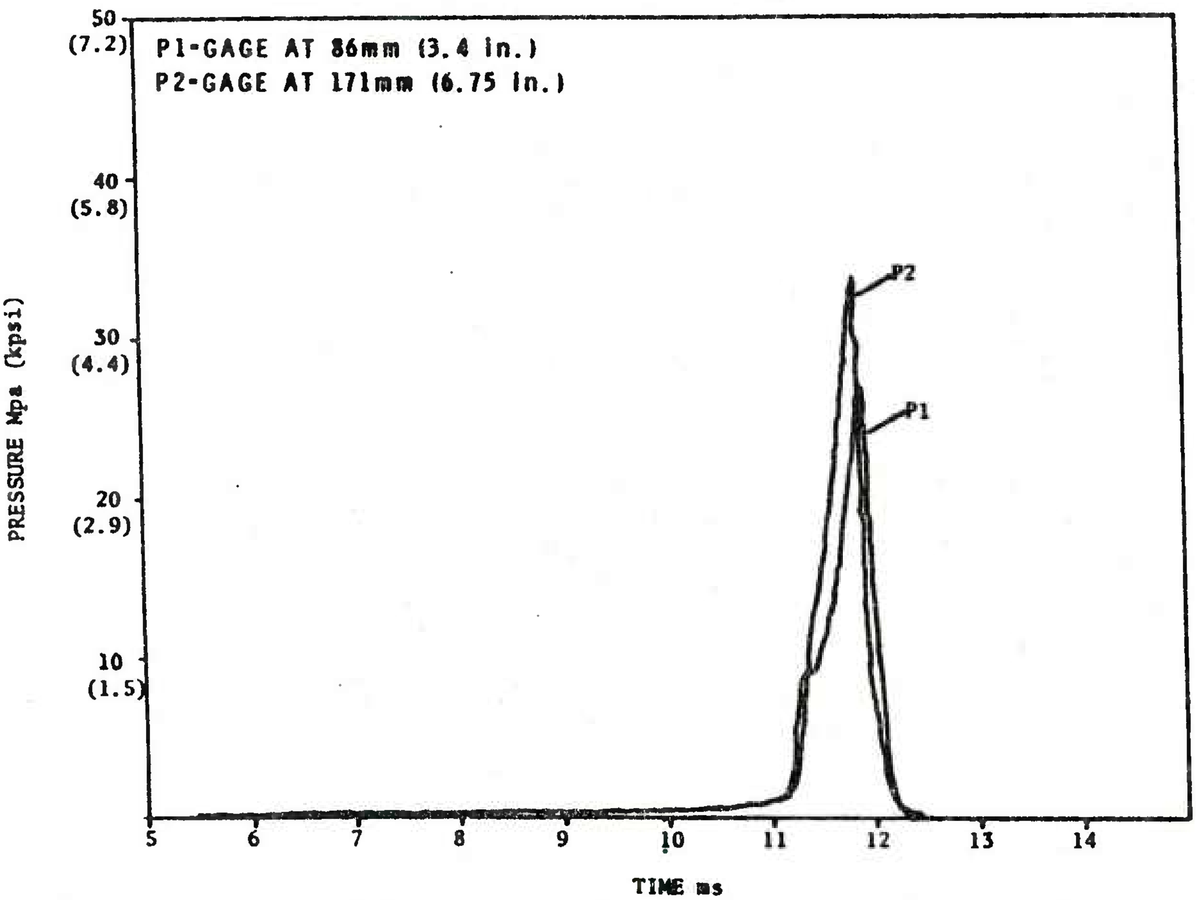

Figure 2. Measured Pressures in the Burning Perforation of a 686-mm (27-in.) Long, Single-Perforated, Unslotted Stick Propellant (M30A1, Lot RAD-PE-472-12) with Unconfined Ignition

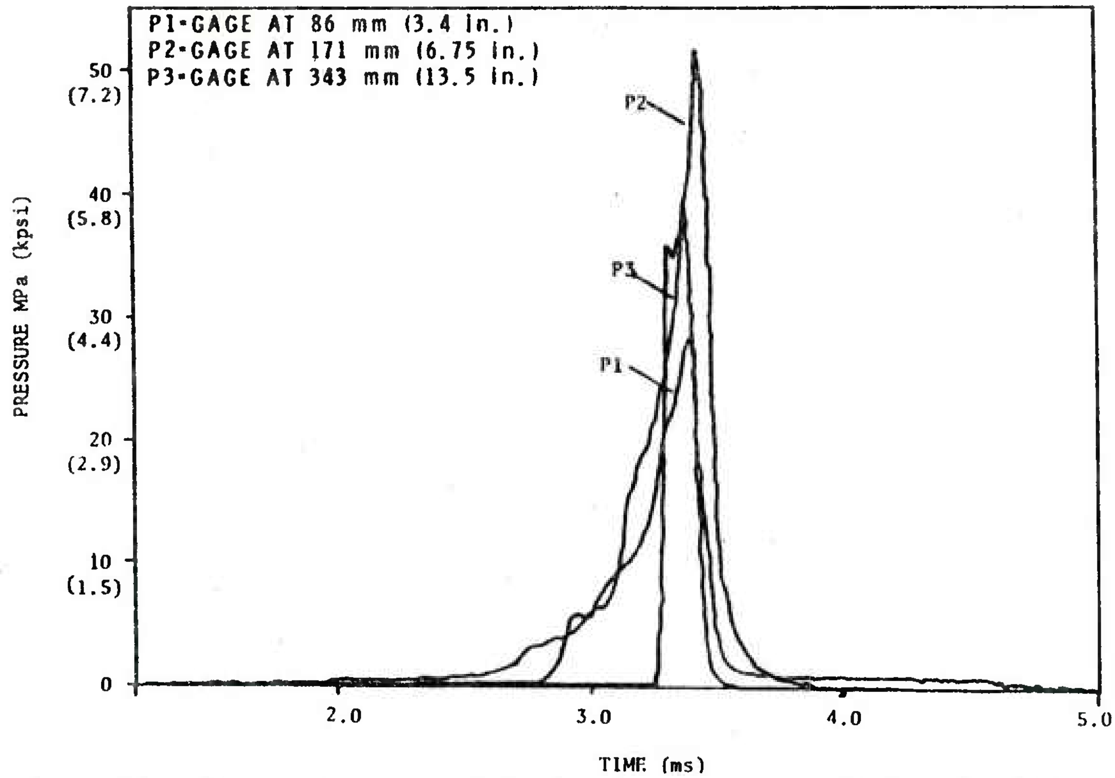

Figure 3. Measured Pressures in the Burning Perforation of a 686-mm (27-in.) Long, Single-Perforated, Unslotted Stick Propellant (M30A1, Lot RAD-PE-472-12) with Confined Ignition

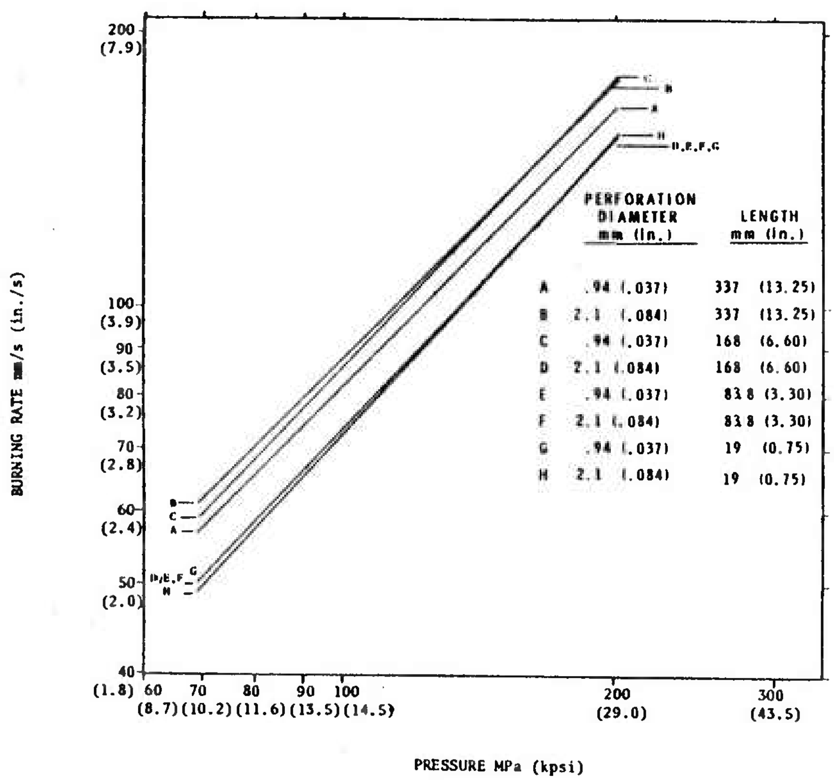

Figure 4. Closed-Bomb Burning Rate Data for 8 Configurations of NOSOL 363 Propellant

A strong dependence on length and on perforation diameter is indicated, with all of the longest grains and those of next greatest length with the smallest perforation diameter exhibiting 15-20 percent higher burning rates than all other samples.

It should be noted that results for the longest grain with the smallest perforation diameter may be somewhat impacted by an inadvertent experimental variable, this test having been performed using a smaller black powder igniter weight.

III. ANALYSIS

Motivated by the disparity between classical predictions and experimental results for stick propellant charge performance, an effort was undertaken to modify the Baer-Frankle lumped-parameter interior ballistic code to treat those processes responsible for the difference.

The first modification incorporated was decoupling of the burning process inside the perforation from that on the exterior surfaces of the stick. This was accomplished by assuming the mass of gas produced inside the perforation was communicated to the exterior free volume in accordance with either sonic or subsonic nozzle flow equations:[8]

$$\frac{dm}{dt} = C\,\pi R^2 P_i \sqrt{\left(\frac{\gamma g}{I}\right)\left(\frac{2}{\gamma + 1}\right)^{\left(\frac{\gamma + 1}{\gamma - 1}\right)}} \tag{1}$$

$$\text{for } P_i > P_o \left(\frac{2}{\gamma + 1}\right)^{\left(\frac{\gamma}{1 - \gamma}\right)}$$

$$\frac{dm}{dt} = C\,\pi R^2 P_i \sqrt{\frac{\gamma g}{I}} \left(\frac{P_i}{P_o}\right)^{\left(\frac{-\gamma - 1}{2\gamma}\right)} \sqrt{\left(\frac{2}{\gamma - 1}\right)\left[\left(\frac{P_i}{P_o}\right)^{\left(\frac{\gamma - 1}{\gamma}\right)} - 1\right]} \tag{2}$$

$$\text{for } P_i < P_o \left(\frac{2}{\gamma + 1}\right)^{\left(\frac{\gamma}{1 - \gamma}\right)}$$

---

[8] *A. S. Shapiro, The Dynamics and Thermodynamics of Compressible Fluid Flow, Ronald Press Company, NY, 1953, Vol I, pp 73-85.*

where:

$\frac{dm}{dt}$ = mass flow rate

γ = interior ballistics gamma

I = impetus

R = radius of perforation

P_i = pressure inside the perforations

P_o = pressure outside of the perforations

g = constant to reconcile units

C = discharge coefficient (correction factor for nonideal behavior)

The analysis requires explicit tracking of separate burning distances inside and outside the perforation since, in general, the two regions will be characterized by different pressure-time histories (i.e., the analysis treats the inside of the grain as a separate component). Further, the nozzle flow area (i.e., perforation diameter) and interior and exterior volumes will be time-dependent. It is also assumed that the perforation has a uniform diameter.

In Figure 5, we see the results of the above analysis incorporated into a current version of the Baer-Frankle lumped-parameter interior ballistic code for different lengths of M30A1 stick propellant. The pressure difference between the inside of the perforation (initial diameter 1.30 mm (0.051 in.))

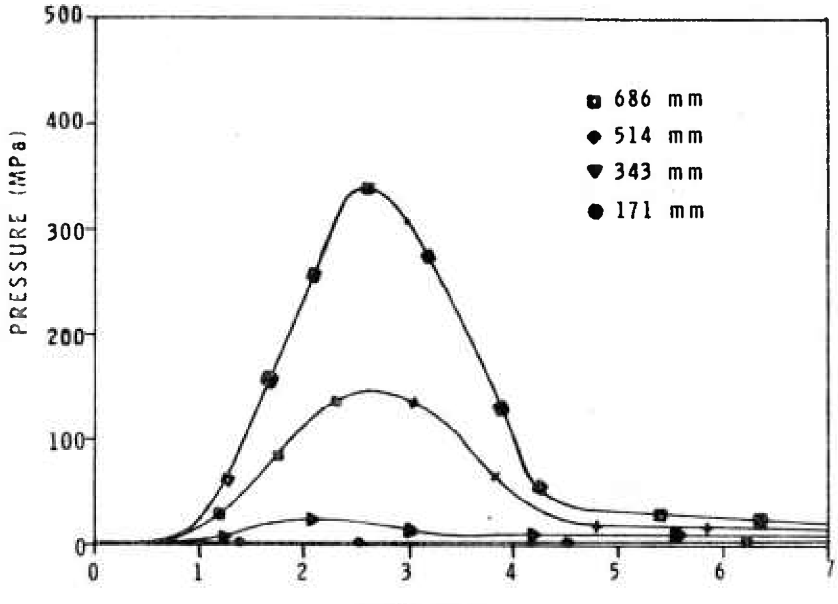

Figure 5. Calculated Pressure Difference Between Stick Propellant Perforation and the Gun Chamber for Varying Stick Lengths

and the gun chamber is plotted as a function of time for lengths 686 mm (27 in.), 514 mm (20.25 in.), 343 mm (13.5 in.), and 171 mm (6.75 in.). All these calculations were done with a discharge coefficient of 1.0. If the discharge coefficient is less than 1.0, then the pressure difference will be larger. It should be noted that there is almost no pressure differential for the 171-mm (6.75-in.) propellant sticks and almost 400 MPa (60 kpsi) for the longest stick. Also, the pressure differential decreases after a few milliseconds as the chamber itself pressurizes.

In Figure 6, results for a stick charge with a constant length of 343 mm (13.5 in.) reveal a strong dependence on perforation diameter as well. Again all calculations were performed with a discharge coefficient of 1.0.

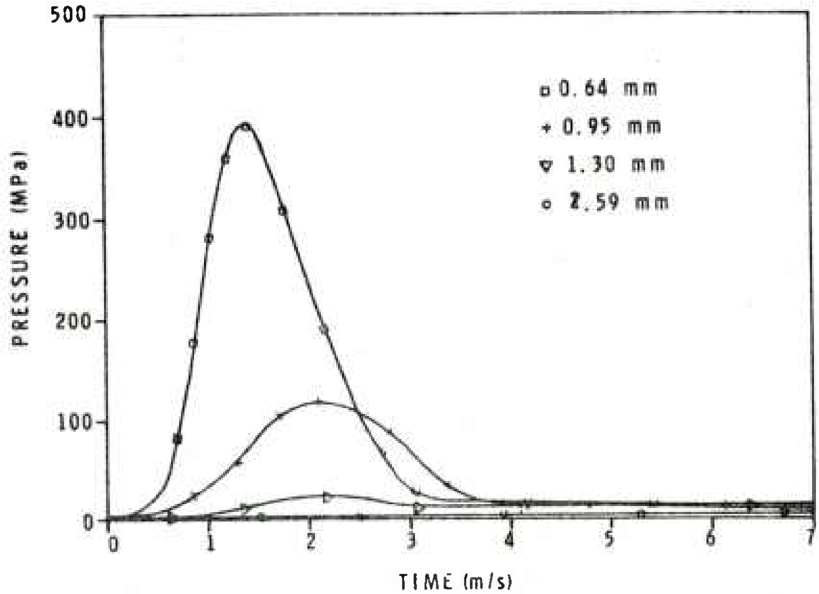

Figure 6. Calculated Pressure Difference Between Stick Propellant Perforation and the Gun Chamber for Varying Stick Perforation Diameters

Figure 7 presents a comparison of maximum chamber pressures predicted by the modified code to the appropriate experimental values from the preceeding section. We note first that, while reasonably good agreement is achieved for short- and full-length sticks, the calculated pressure for intermediate length sticks is quite low in comparison to available data. Second, it is evident from the analysis (though not observable in the figure) that the pressure differential between the interior of the perforation and exterior to the grain exceeds the dynamic burst pressure for most firing conditions.

Therefore, a fracture criterion, based on a simple pressure differential independent of wall thickness, was implemented in the modified code. When the criterion is met, the separate analysis for burning inside the perforations is discontinued. An apparent surface area increase due to fracture is then effected by reducing effective web for the duration of the calculation. In these calculations, the magnitude of this area increase was established by normalization of predicted maximum chamber pressure to the experimental value for the full-length grains. The full-length case was adopted for normalization since rapid internal pressurization rates rendered it least sensitive to values for discharge coefficient and fracture pressure.

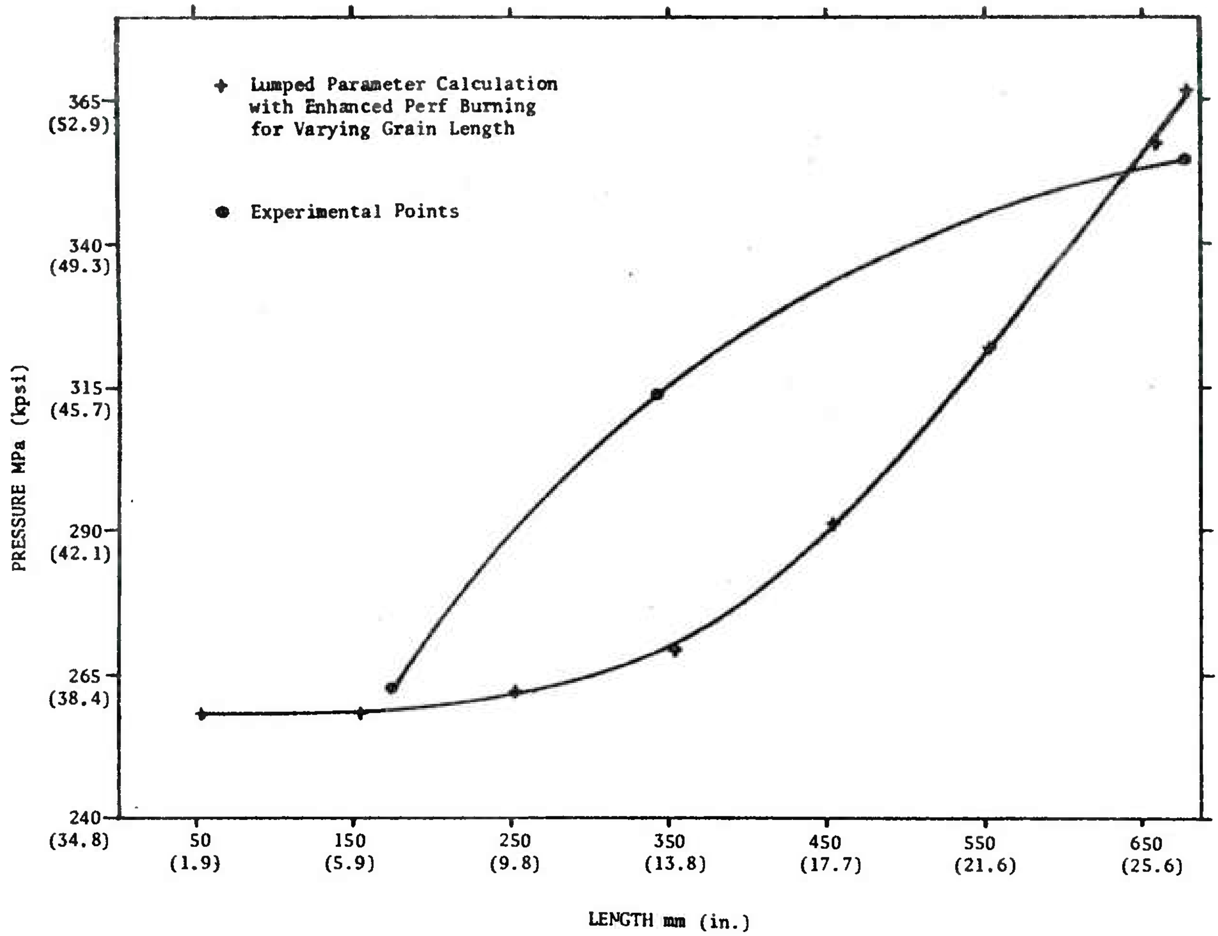

Figure 7. Calculated and Experimental Points of the Maximum Chamber Pressure for a 155-mm (M199 Cannon) Howitzer

For the full-length sticks, a surface area increase of 27 percent (effected by a 21-percent decrease in web) resulted in the experimentally observed maximum chamber pressure of 354 MPa (51.3 kpsi). However, with the same discharge coefficient of 1.0, the 343-mm (13.5-in.) sticks were not predicted to fracture. Reducing the discharge coefficient to 0.9 led to a predicted fracture, but the accompanying predicted chamber pressure rose from 269 MPa (39 kpsi) to 352 MPa (51 kpsi) rather than the experimentally observed value of 314 MPa (45.5 kpsi).

Next, a fracture criterion based on hoop stress, both with and without time-dependence of the wall thickness, was evaluated with the same lack of success.

Finally, the perhaps physically more well-motivated Lamé equation for thick-wall cylinders[9] was implemented:

[9] *Timoshenko and Goodier, Theory of Elasticity, McGraw-Hill Book Company, NY, 1951, pp 55-60.*

$$\sigma_\theta = \frac{a^2 b^2 (P_i - P_o)}{b^2 - a^2} \cdot \frac{1}{r^2} + \frac{P_i a^2 - P_o b^2}{b^2 - a^2} \qquad (3)$$

where:

σ_θ = tangential stress at distance r

a = inside radius of tube

b = outside radius of tube

P_i = pressure inside tube

P_o = pressure outside tube

r = radial distance at which stress is calculated

Using the fracture pressures defined in Table 4, assuming the largest stress occurs at the inner surface (r = a), and assuming P_o (atmospheric for the fracture tests) << P_i, we can define the tangential stress at fracture:

$$\sigma_{\theta_f} = \frac{P_i (b^2 + a^2)}{b^2 - a^2} \qquad (4)$$

When P_o is large, as in the gun environment, this becomes

$$\sigma_{\theta_f} \cdot \frac{(b^2 - a^2)}{b^2} = P_i + P_i(\frac{a^2}{b^2}) - 2P_o \qquad (5)$$

where $P_i + P_i(\frac{a^2}{b^2}) - 2P_o$ must exceed $\sigma_{\theta_f} (\frac{b^2 - a^2}{b^2})$ for grain fracture. Here, the values of a and b are the instantaneous values of inner and outer radii, which change as the grain burns. This formulism suggests that the effective pressure differential to cause fracture in the gun environment should be greater than indicated by the atmospheric tests, rendering even more difficult our task of properly defining a fracture criterion that will lead to prediction of experimentally observed gun pressures for all propellant lengths.

Clearly, some additional insight was needed to properly account for the observed performance depicted in Figure 7. It had been observed in the open-air, grain-fracture experiments that fracture occurred leaving the ends of the sticks often still intact. Such behavior might be expected to lead to a proportionally smaller increase in surface area the shorter the stick. Indeed, when increase in surface area upon fracture for the 343-mm (13.5-in.) sticks was decreased from 27 percent to 18 percent, the desired prediction of a 314 MPa (45.5 kpsi) maximum chamber pressure was achieved. Naturally, predictions for the shorter grains, not predicted to fracture, remained unaltered and correct.

It would appear equally plausible that the critical σ_θ for fracture might be dependent on the duration of the applied stress, offering another option worthy of investigation.

Calculations were also performed using an experimental version of the NOVA code,[7] in which flow within the perforations is treated explicitly and separately from the exterior of the sticks. This code employs an ignition criterion based on surface temperature and provides a full continuum description of all flow variables (i.e., pressure, temperature, density, and velocity).

As can be seen from results depicted in Figure 8, the pressure in the perforation for a long, single-perforated, unslotted stick of M30A1 propellant is calculated to rise 140 MPa (20 kpsi) in 1.6 ms, while the exterior pressure has risen only 7 MPa (1 kpsi). This time frame for pressurization of the perforation is consistent with the experimental data of Figures 2 and 3. The maximum pressure in the perforation from the NOVA calculations is about 329 MPa (47.7 kpsi), while the maximum pressure calculated with the lumped-parameter code is 358 MPa (51.9 kpsi). (See Figure 6.)

The time between ignition of the outer surfaces and the surfaces within the perforations is predicted by NOVA to be about 1 ms. This short delay appears to support the assumption of instantaneous ignition typically used in lumped-parameter codes.

IV. CONCLUSIONS

A simple model of stick propellant combustion has been devised which accounts for augmented burning within the perforations of long, unslotted stick propellant, a consequence of higher local pressures resulting from choked flow of the exiting gases. Calculations performed using this model predict large pressure differentials between the perforation and exterior of the stick which, for some configurations, seem likely to lead to propellant fracture.

Companion experiments, in which the perforations of various stick propellants were pressurized both quasi-statically and dynamically, confirm that grain fracture is probable and must be accounted for in the model.

A simple propellant fracture criterion based on the Lamé equation was implemented and evaluated in the above model. It was found, however, that an ad hoc prescription of fracture surface was required to provide complete agreement between theory and experiment.

Additional calculations performed using a modified version of the NOVA code to provide a continuum description of flow within the perforations suggest extremely rapid flamespreading on internal surfaces of long propellant sticks. This result lends support to the adequacy of the assumption of instantaneous ignition of all surfaces employed in the simpler codes.

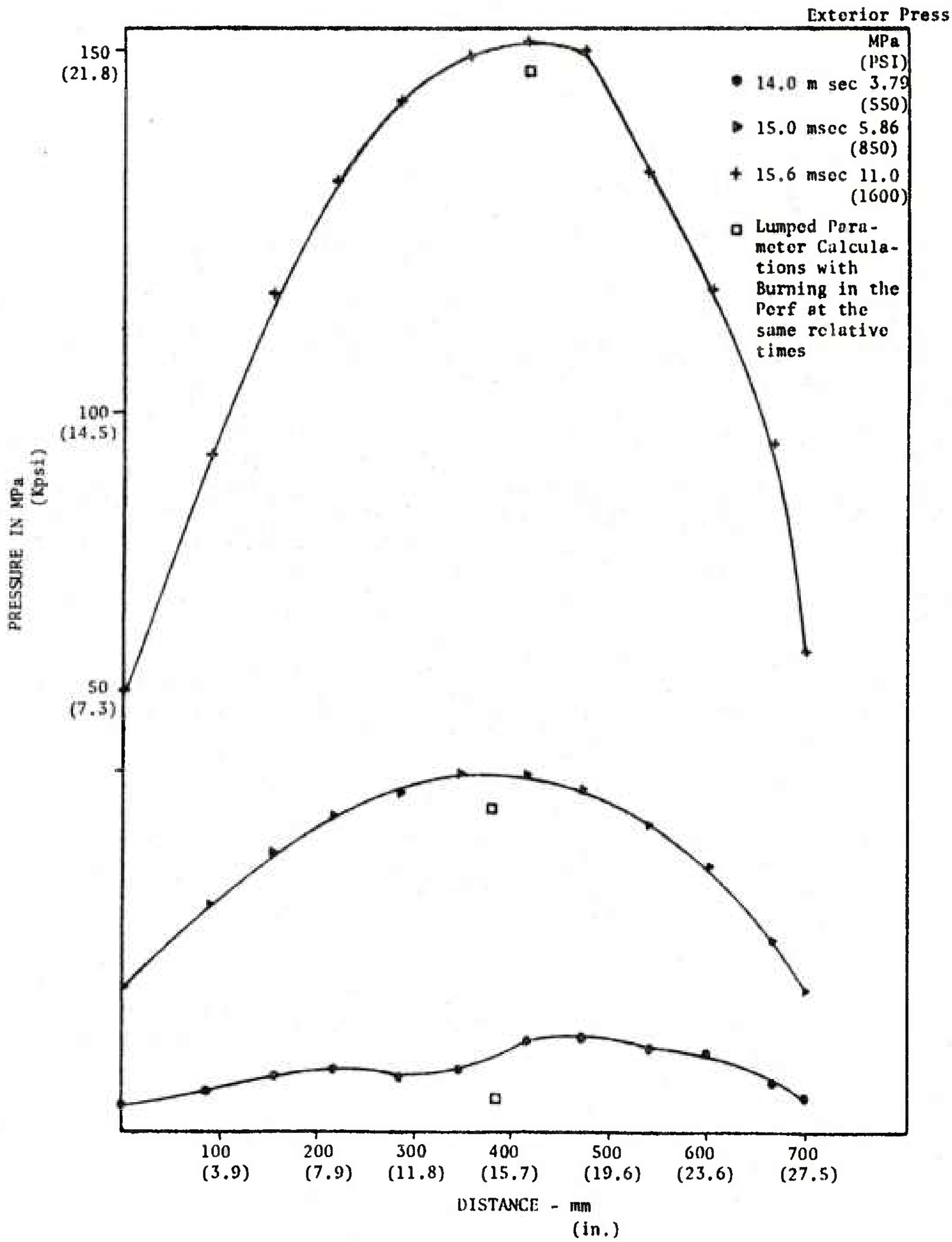

Figure 8. NOVA Code Calculations for Pressure in the Perforations of 686-mm (27-in.) Long, Single-Perforated, Unslotted Stick Propellant (M30A1, Lot RAD-PE-472-12)

V. RECOMMENDATIONS

1. Further experimentation should be carried out to quantify the rate dependence of propellant fracture phenomena.

2. Tests must be performed in blowout or short-barreled gun fixtures which allow the collection of extinguished propellant sticks to validate the hypothesis of grain fracture.

3. Investigation of the influence of igniter characteristics on subsequent ignition and burning in the perforations of stick propellant should be pursued.

4. Further fracture testing of various lengths of stick propellant should be undertaken to gain information about relative increases in surface area.

ACKNOWLEDGMENTS

The authors wish to thank Mr. R. S. Westley, LCWSL, USA ARRADCOM, Dover, NJ, for providing the two M30A1 stick propellants. Appreciation is also expressed to Mr. T. C. Smith, Naval Ordnance Station, Indian Head, MD, for manufacturing and providing the two NOSOL 363 stick propellants and for furnishing a copy of the experimental version of the NOVA code. We also wish to thank Dr. A. A. Juhasz, Ballistic Research Laboratory, USA ARRADCOM, Aberdeen Proving Ground, MD, for performing the closed-bomb firings of the NOSOL 363 propellants.

REFERENCES

1. F. W. Robbins, J. A. Kudzal, J. A. McWilliams, and P. S. Gough, "Experimental Determination of Stick Charge Flow Resistance," 17th JANNAF Combustion Meeting, CPIA Publication 329, Vol II, pp 97-118, November 1980.

2. T. C. Smith, "Experimental Gun Testing of High Density Multi-Perforated Stick Propellant Charge Assemblies," 17th JANNAF Combustion Meeting, CPIA Publication 329, Vol II, pp 87-98, November 1980.

3. A. Grabowsky, S. Weiner, and A. Beardell, "Closed Bomb Testing of Stick Propellant for Gun Firing Simulation," 17th JANNAF Combustion Meeting, CPIA Publication 329, Vol II, pp 119-124, November 1980.

4. A. W. Horst and T. C. Minor, "Improved Flow Dynamics in Guns Through the Use of Alternative Propellant Grain Geometries," 1980 JANNAF Propulsion Meeting, CPIA Publication 315, Vol I, pp 325-352, March 1980.

5. S. Weiner, "Investigation of Stick Propellant for 155-mm Howitzer XM198," Interim Memorandum Report, Picatinny Arsenal, Dover, New Jersey, July 1975.

6. P. G. Baer and J. M. Frankle, "The Simulation of Interior Ballistic Performance of Guns by Digital Computer Program," BRL R 1183, USA Aberdeen Research and Development Center, Ballistic Research Laboratories, Aberdeen Proving Ground, MD, December 1962 (AD 299980).

7. P. S. Gough, "Extensions to NOVA Flamespreading Modeling Capacity," Task I Report for the Naval Ordnance Station, Indian Head, MD, Contract N00174-80-C-0316, Paul Gough Associates, Inc., Portsmouth, NH, April 1981.

8. A. S. Shapiro, The Dynamics and Thermodynamics of Compressible Fluid Flow, Ronald Press Company, NY, 1953, Vol I, pp 73-85.

9. Timoshenko and Goodier, Theory of Elasticity, McGraw-Hill Book Company, NY, 1951, pp 55-60.

DISTRIBUTION LIST

No. Of Copies	Organization
12	Administrator Defense Technical Info Center ATTN: DTIC-DDA Cameron Station Alexandria, VA 22314
1	Office of the Under Secretary of Defense Research & Engineering ATTN: R. Thorkildsen Washington, DC 20301
1	HQDA/SAUS-OR, D. Hardison Washington, DC 20301
1	HQDA/DAMA-ZA Washington, DC 20310
1	HQDA, DAMA-CSM, E. Lippi Washington, DC 20310
1	HQDA/SARDA Washington, DC 20310
1	Commandant US Army War College ATTN: Library-FF229 Carlisle Barracks, PA 17013
1	Commander US Army BMD Advanced Tech Cntr P. O. Box 1500 Huntsville, AL 35804
1	Chairman DOD Explosives Safety Board Room 856-C Hoffman Bldg. 1 2461 Eisenhower Avenue Alexandria, VA 22331
3	Commander US Army Materiel Development and Readiness Command ATTN: DRCDMD-ST DCRSF-E, Safety Office DRCDE-DW 5001 Eisenhower Avenue Alexandria, VA 22333
13	Commander US Army Armament R&D Command ATTN: DRDAR-TD, A. Moss DRDAR-TSS (2 cys) DRDAR-TDC D. Gyorog DRDAR-LCA J. Lannon A. Beardell D. Downs S. Einstein L. Schlosberg S. Westley S. Bernstein P. Kemmey C. Heyman Dover, NJ 07801
9	US Army Armament R&D Command ATTN: DRDAR-SCA, L. Stiefel B. Brodman DRDAR-LCB-I, D. Spring DRDAR-LCE, R. Walker DRDAR-LCU-CT E. Barrieres R. Davitt DRDAR-LCU-CV C.Mandala E. Moore DRDAR-LCM-E S. Kaplowitz Dover, NJ 07801

DISTRIBUTION LIST

No. Of Copies	Organization
1	Commander US Army Armament R&D Command ATTN: DRDAR-QAR, J. Rutkowski Dover, NJ 07801
5	Project Manager Cannon Artillery Weapons System ATTN: DRCPM-CW, F. Menke DRCPM-CWW H. Noble DRCPM-CWS M. Fisette DRCPM-CWA R. DeKleine H. Hassmann Dover, NJ 07801
2	Project Manager Munitions Production Base Modernization and Expansion ATTN: DRCPM-PMB, A. Siklosi SARPM-PBM-E, L. Laibson Dover, NJ 07801
3	Project Manager Tank Main Armament System ATTN: DRCPM-TMA, K. Russell DRCPM-TMA-105 DRCPM-TMA-120 Dover, NJ 07801
3	Commander US Army Armament R&D Command ATTN: DRDAR-LCW-A M.Salsbury DRDAR-LCS DRDAR-LC, J. Frasier Dover, NJ 07801
5	Commander US Army Armament Materiel Readiness Command ATTN: DRSAR-LEP-L, DRSAR-LC, L. Ambrosini DRSAR-IRC, G. Cowan DRSAR-LEM, W. Fortune R. Zastrow Rock Island, IL 61299
1	Commander US Army Watervliet Arsenal ATTN: SARWV-RD, R. Thierry Watervliet, NY 12189
1	Director US Army ARRADCOM Benet Weapons Laboratory ATTN: DRDAR-LCB-TL Watervliet, NY 12189
1	Commander US Army Aviation Research and Development Command ATTN: DRDAV-E 4300 Goodfellow Blvd. St. Louis, MO 63120
1	Commander US Army TSARCOM 4300 Goodfellow Blvd. St. Louis, MO 63120
1	Director US Army Air Mobility Research And Development Laboratory Ames Research Center Moffett Field, CA 94035

DISTRIBUTION LIST

No. Of Copies	Organization	No. Of Copies	Organization
1	Commander US Army Communications Research and Development Command ATTN: DRSEL-ATDD Fort Monmouth, NJ 07703	1	Project Manager Improved TOW Vehicle ATTN: DRCPM-ITV Warren MI 48090
1	Commander US Army Electronics Research and Development Command Technical Support Activity ATTN: DELSD-L Fort Monmouth, NJ 07703	1	Program Manager M1 Abrams Tank System ATTN: DRCPM-GMC-SA Warren, MI 48090
1	Commander US Army Harry Diamond Lab. ATTN: DELHD-TA-L 2800 Powder Mill Road Adelphi, MD 20783	1	Project Manager Fighting Vehicle Systems ATTN: DRCPM-FVS Warren, MI 48090
2	Commander US Army Missile Command ATTN: DRSMI-R DRSMI-YDL Redstone Arsenal, AL 35898	1	Director US Army TRADOC Systems Analysis Activity ATTN: ATAA-SL White Sands Missile Range NM 88002
1	Commander US Army Natick Research and Development Command ATTN: DRDNA-DT, D. Sieling Natick, MA 01762	1	Project Manager M-60 Tank Development ATTN: DRCPM-M60TD Warren, MI 48090
1	Commander US Army Tank Automotive Command ATTN: DRSTA-TSL Warren, MI 48090	1	Commander US Army Training & Doctrine Command ATTN: ATCD-A/MAJ Williams Fort Monroe, VA 23651
1	US Army Tank Automotive Materiel Readiness Command ATTN: DRSTA-CG Warren, MI 48090	2	Commander US Army Materials and Mechanics Research Center ATTN: DRXMR-ATL Tech Library Watertown, MA 02172

DISTRIBUTION LIST

No. Of Copies	Organization
1	Commander US Army Research Office ATTN: Tech Library P. O. Box 12211 Research Triangle Park, NC 27709
1	Commander US Army Mobility Equipment Research & Development Command ATTN: DRDME-WC Fort Belvoir, VA 22060
1	Commander US Army Logistics Mgmt Ctr Defense Logistics Studies Fort Lee, VA 23801
2	Commandant US Army Infantry School ATTN: ATSH-CD-CSO-OR Fort Benning, GA 31905
1	US Army Armor & Engineer Board ATTN: STEBB-AD-S Fort Knox, KY 40121
1	Commandant US Army Aviation School ATTN: Aviation Agency Fort Rucker, AL 36360
1	Commandant Command and General Staff College Fort Leavenworth, KS 66027
1	Commandant US Army Special Warfare School ATTN: Rev & Tng Lit Div Fort Bragg, NC 28307
1	Commandant US Army Engineer School ATTN: ATSE-CD Ft. Belvoir, VA 22060
1	Commander US Army Foreign Science & Technology Center ATTN: DRXST-MC-3 220 Seventh Street, NE Charlottesville, VA 22901
1	President US Army Artillery Board Ft. Sill, OK 73504
1	Commandant US Army Field Artillery School ATTN: ATSF-CO-MW, B. Willis Ft. Sill, OK 73503
3	Commandant US Army Armor School ATTN: ATZK-CD-MS M. Falkovitch Armor Agency Fort Knox, KY 40121
1	Chief of Naval Materiel Department of the Navy ATTN: J. Amlie Washington, DC 20360
1	Office of Naval Research ATTN: Code 473, R. S. Miller 800 N. Quincy Street Arlington, VA 22217
2	Commander Naval Sea Systems Command ATTN: SEA-62R, J. W. Murrin R. Beauregard National Center, Bldg. 2 Room 6E08 Washington, DC 20360
1	Commander Naval Air Systems Command ATTN: NAIR-954-Tech Lib Washington, DC 20360

DISTRIBUTION LIST

No. Of Copies	Organization
1	Strategic Systems Project Office Dept. of the Navy Room 901 ATTN: J. F. Kincaid Washington, DC 20376
1	Assistant Secretary of the Navy (R, E, and S) ATTN: R. Reichenbach Room 5E787 Pentagon Bldg. Washington, DC 20350
1	Naval Research Lab Tech Library Washington, DC 20375
5	Commander Naval Surface Weapons Center ATTN: Code G33, J. L. East W. Burrell J. Johndrow Code G23, D. McClure Code DX-21 Tech Lib Dahlgren, VA 22448
2	Commander US Naval Surface Weapons Center ATTN: J. P. Consaga C. Gotzmer Indian Head, MD 20640
4	Commander Naval Surface Weapons Center ATTN: S. Jacobs/Code 240 Code 730 K. Kim/Code R-13 R. Bernecker Silver Spring, MD 20910
2	Commanding Officer Naval Underwater Systems Center Energy Conversion Dept. ATTN: CODE 5B331, R. S. Lazar Tech Lib Newport, RI 02840
4	Commander Naval Weapons Center ATTN: Code 388, R. L. Derr C. F. Price T. Boggs Info. Sci. Div. China Lake, CA 93555
2	Superintendent Naval Postgraduate School Dept. of Mechanical Engineering ATTN: A. E. Fuhs Code 1424 Library Monterey, CA 93940
6	Commander Naval Ordnance Station ATTN: P. L. Stang J. Birkett S. Mitchell C. Christensen D. Brooks Tech Library Indian Head, MD 20640
1	AFSC/SDOA Andrews AFB Washington, DC 20334
1	Program Manager AFOSR Directorate of Aerospace Sciences ATTN: L. H. Caveny Bolling AFB, DC 20332
6	AFRPL (DYSC) ATTN: D. George J. N. Levine B. Goshgarian D. Thrasher N. Vander Hyde Tech Library Edwards AFB, CA 93523
1	AFWL/SUL Kirtland AFB, NM 87117

DISTRIBUTION LIST

No. Of Copies	Organization
1	AFFTC ATTN: SSD-Tech LIb Edwards AFB, CA 93523
1	AFATL ATTN: DLYV Eglin AFB, FL 32542
1	AFATL/DLDL ATTN: O. K. Heiney Eglin AFB, FL 32542
1	ADTC ATTN: DLODL Tech Lib Eglin AFB, FL 32542
1	AFFDL ATTN: TST-Lib Wright-Patterson AFB, OH 45433
1	NASA HQ 600 Independence Avenue, SW ATTN: Code JM6, Tech Lib. Washington, DC 20546
1	NASA/Lyndon B. Johnson Space Center ATTN: NHS-22, Library Section Houston, TX 77058
1	Aerodyne Research, Inc. Bedford Research Park ATTN: V. Yousefian Bedford, MA 01730
1	Aerojet Solid Propulsion Co. ATTN: P. Micheli Sacramento, CA 95813

No. Of Copies	Organization
1	AVCO Everett Rsch Lab ATTN: D. Stickler 2385 Revere Beach Parkway Everett, MA 02149
2	Calspan Corporation ATTN: Tech Library P. O. Box 400 Buffalo, NY 14225
1	Foster Miller Associates ATTN: A. Erickson 135 Second Avenue Waltham, MA 02154
1	Atlantic Research Corporation ATTN: M. K. King 5390 Cherokee Avenue Alexandria, VA 22314
1	General Applied Sciences Lab ATTN: J. Erdos Merrick & Stewart Avenues Westbury Long Island, NY 11590
1	General Electric Company Armament Systems Dept. ATTN: M. J. Bulman, Room 1311 Lakeside Avenue Burlington, VT 05412
1	Hercules, Inc. Allegheny Ballistics Laboratory ATTN: R. B. Miller P. O. Box 210 Cumberland, MD 21501
1	Hercules, Inc Bacchus Works ATTN: K. P. McCarty P. O. Box 98 Magna, UT 84044

DISTRIBUTION LIST

No. Of Copies	Organization
1	Hercules, Inc. Eglin Operations AFATL DLDL ATTN: R. L. Simmons Eglin AFB, FL 32542
1	IITRI ATTN: M. J. Klein 10 W. 35th Street Chicago, IL 60616
2	Lawrence Livermore Laboratory ATTN: M. S. L-355, A. Buckingham M. Finger P. O. Box 808 Livermore, CA 94550
1	Olin Corporation Badger Army Ammunition Plant ATTN: R. J. Thiede Baraboo, WI 53913
1	Olin Corporation Smokeless Powder Operations ATTN: R. L. Cook P. O. Box 222 St. Marks, FL 32355
1	Paul Gough Associates, Inc. ATTN: P. S. Gough 1048 South Street Portsmouth, NH 03801
1	Physics International 2700 Merced Street San Leandro, CA 94577
1	Princeton Combustion Research Lab., Inc. ATTN: M. Summerfield 1041 US Highway One North Princeton, NJ 08540

No. Of Copies	Organization
2	Rockwell International Rocketdyne Division ATTN: BA08 J. E. Flanagan J. Grey 6633 Canoga Avenue Canoga Park, CA 91304
1	Science Applications, Inc. ATTN: R. B. Edelman 23146 Cumorah Crest Woodland Hills, CA 91364
1	Scientific Research Assoc., Inc. ATTN: H. McDonald P. O. Box 498 Glastonbury, CT 06033
2	Thiokol Corporation Elkton Division ATTN: R. Biddle Tech Library P.O. Box 358 Elkton, MD 21921
3	Thiokol Corporation Huntsville Division ATTN: D. Flanigan R. Glick Tech Library Huntsville, AL 35807
2	Thiokol Corporation Wasatch Division ATTN: J. Peterson Tech Library P. O. Box 524 Brigham City, UT 84302

DISTRIBUTION LIST

No. Of Copies	Organization
2	United Technologies Chemical Systems Division ATTN: R. Brown Tech Library P. O. Box 358 Sunnyvale, CA 94086
1	Universal Propulsion Company ATTN: H. J. McSpadden Black Canyon Stage 1 Box 1140 Phoenix, AZ 85029
1	Veritay Technology, Inc. ATTN: E. B. Fisher P. O. Box 22 Bowmansville, NY 14026
1	Southwest Research Institute Institute Scientists ATTN: Robert E. White 8500 Culebra Road San Antonio, TX 78228
1	Battelle Memorial Institute ATTN: Tech Library 505 King Avenue Columbus, OH 43201
1	Brigham Young University Dept. of Chemical Engineering ATTN: M. Beckstead Provo, UT 84601
1	California Institute of Tech 204 Karman Lab Main Stop 301-46 ATTN: F. E. C. Culick 1201 E. California Street Pasadena, CA 91125
1	California Institute of Tech Jet Propulsion Laboratory 4800 Oak Grove Drive Pasadena, CA 91103

No. Of Copies	Organization
1	University of Illinois Dept. of Mech. Eng. ATTN: H. Krier 144 MEB, 1206 W. Green St. Urbana, IL 61801
1	University of Massachusetts Dept. of Mechanical Engineering ATTN: K. Jakus Amherst, MA 01002
1	University of Minnesota Dept. of Mechanical Engineering ATTN: E. Fletcher Minneapolis, MN 55455
1	Case Western Reserve University Division of Aerospace Sciences ATTN: J. Tien Cleveland, OH 44135
3	Georgia Institute of Tech School of Aerospace Eng. ATTN: B. T. Zinn E. Price W. C. Strahle Atlanta, GA 30332
1	Institute of Gas Technology ATTN: D. Gidaspow 3424 S. State Street Chicago, IL 60616
1	Johns Hopkins University Applied Physics Laboratory Chemical Proplsion Information Agency ATTN: T. Christian Johns Hopkins Road Laurel, MD 20707

DISTRIBUTION LIST

No. Of Copies	Organization
1	Massachusetts Institute of Technology Dept of Mechanical Engineering ATTN: T. Toong Cambridge, MA 02139
1	Pennsylvania State University Applied Research Lab ATTN: G. M. Faeth P. O. Box 30 State College, PA 16801
1	Pennsylvania State University Dept. Of Mechanical Engineering ATTN: K. Kuo University Park, PA 16802
1	Purdue University School of Mechanical Engineering ATTN: J. R. Osborn TSPC Chaffee Hall West Lafayette, IN 47906
1	Rensselaer Polytechnic Inst. Department of Mathematics Troy, NY 12181
1	Rutgers University Dept. of Mechanical and Aerospace Engineering ATTN: S. Temkin University Heights Campus New Brunswick, NJ 08903
1	SRI International Propulsion Sciences Division ATTN: Tech Library 333 Ravenswood Avenue Menlo Park, CA 94025
1	Stevens Institute of Technology Davidson Laboratory ATTN: R. McAlevy, III Hoboken, NJ 07030

No. Of Copies	Organization
2	Los Alamos National Lab ATTN: T. D. Butler, MS B216 M. Division, B. Craig P. O. Box 1663 Los Alamos, NM 87545
1	University of Southern California Mechanical Engineering Dept. ATTN: OHE200, M. Gerstein Los Angeles, CA 90007
2	University of Utah Dept. of Chemical Engineering ATTN: A. Baer G. Flandro Salt Lake City, UT 84112
1	Washington State University Dept. of Mechanical Engineering ATTN: C. T. Crowe Pullman, WA 99163

Aberdeen Proving Ground

Dir, USAMSAA
ATTN: DRXSY-D
DRXSY-MP, H. Cohen
Cdr, USATECOM
ATTN: DRSTE-TO-F
STEAP-MT, S. Walton
G. Rice
D. Lacey
C. Herud
Dir, HEL
ATTN: J. Weisz
Dir, USACSL, Bldg. E3526, EA
ATTN: DRDAR-CLB-PA
DRDAR-CLN
DRDAR-CLJ-L

USER EVALUATION OF REPORT

Please take a few minutes to answer the questions below; tear out this sheet, fold as indicated, staple or tape closed, and place in the mail. Your comments will provide us with information for improving future reports.

1. BRL Report Number ______________________

2. Does this report satisfy a need? (Comment on purpose, related project, or other area of interest for which report will be used.)

____

____

____

3. How, specifically, is the report being used? (Information source, design data or procedure, management procedure, source of ideas, etc.) ______________________

____

____

4. Has the information in this report led to any quantitative savings as far as man-hours/contract dollars saved, operating costs avoided, efficiencies achieved, etc.? If so, please elaborate.

____

____

5. General Comments (Indicate what you think should be changed to make this report and future reports of this type more responsive to your needs, more usable, improve readability, etc.) ______________________

____

____

____

6. If you would like to be contacted by the personnel who prepared this report to raise specific questions or discuss the topic, please fill in the following information.

Name: ______________________

Telephone Number: ______________________

Organization Address: ______________________

____

____